Appl. Phys. B 81, 585–588 (2005)
DOI: 10.1007/s00340-005-1929-8

Applied Physics B
Lasers and Optics

E.E. SEREBRYANNIKOV[1]
A.M. ZHELTIKOV[1,✉]
N. ISHII[2]
C.Y. TEISSET[2]
S. KÖHLER[2]
T. FUJI[2]
T. METZGER[2]
F. KRAUSZ[2,3]
A. BALTUŠKA[2]

Soliton self-frequency shift of 6-fs pulses in photonic-crystal fibers

[1]Physics Department, International Laser Center, M. V. Lomonosov Moscow State University, Vorob'evy gory, Moscow 119992, Russia
[2]Max-Planck-Institut für Quantenoptik, Hans-Kopfermann-Strasse 1, 85748 Garching, Germany
[3]Department für Physik, Ludwig-Maximilians-Universität Munich, 85748 Garching, Germany

Received: 14 June 2005
Published online: 18 August 2005 •

ABSTRACT Raman soliton phenomena in photonic crystal fibers are shown to allow efficient tunable frequency shifting of sub-10-fs laser pulses. Soliton self-frequency shift in a photonic-crystal fiber with a core diameter less than 2 μm is used to transform the spectrum of a 6-fs 2-nJ Ti: sapphire-laser pulse, dominated by a 670-nm peak, into a spectrum featuring a well-resolved intense spectral component centered at 1064 nm, which is ideally suited as a seed for Nd: YAG- and ytterbium-based laser devices.

PACS 42.65.Wi; 42.81.Qb

Optical solitons propagating in media with non-instantaneous nonlinear response experience reshaping and continuous frequency down-shifting due to the Raman effect [1]. This phenomenon, called soliton self-frequency shift (SSFS) [2, 3], provides a convenient way of generating ultrashort pulses with a tunable carrier frequency. Photonic-crystal fibers (PCFs) [4] can substantially enhance this nonlinear-optical process due to a strong field confinement in a small-size fiber core and the possibility to tailor dispersion of guided modes by varying the fiber structure [5]. As shown by Liu et al. [6], a 15-cm of PCF can provide an SSFS of up to 20% of the carrier frequency of 200-fs input pulses with the initial carrier wavelength of 1.3 μm. PCFs thus offer attractive recipes for the creation of highly efficient SSFS-based frequency shifters [7–10].

Input pulse duration is one of the key parameters controlling the soliton dynamics in the SSFS regime. As demonstrated by Gordon [11], the SSFS rate $\mathrm{d}\nu/\mathrm{d}z$, where ν is the carrier frequency and z is the propagation coordinate, rapidly grows with a decrease in the pulse duration τ_0. With a linear approximation of the Raman gain as a function of the frequency, the integration of the nonlinear Schrödinger equation yields $\mathrm{d}\nu/\mathrm{d}z \propto \tau_0^{-4}$. Although high-order dispersion and deviations of the Raman gain curve from the linear dependence generally make the relation between $\mathrm{d}\nu/\mathrm{d}z$ and τ in soliton dynamics more complicated, SSFS strategies seem to offer much promise for the frequency shifting of extremely short laser pulses and few-cycle field waveforms, especially in combination with the tailored dispersion of PCFs.

In this work, we explore the potential of SSFS in PCFs for the spectral transformation of 6-fs laser pulses. We theoretically predict and experimentally demonstrate that SSFS in a PCF with a special dispersion profile can transform the spectrum of a 6-fs 2-nJ Ti:sapphire-laser pulse, dominated by a 670-nm peak, into a spectrum featuring a well-resolved intense spectral component centered at 1064 nm.

Our theoretical analysis of propagation of laser pulses in PCFs was based on the numerical solution of the generalized nonlinear Schrödinger equation [1]

$$\frac{\partial A}{\partial z} = \mathrm{i}\sum_{\mathrm{k}=2}^{6} \frac{(\mathrm{i})^{\mathrm{k}}}{k!}\,\beta^{(\mathrm{k})}\frac{\partial^{\mathrm{k}} A}{\partial \tau^{\mathrm{k}}} + \mathrm{i}\gamma\left(1+\frac{\mathrm{i}}{\omega_0}\frac{\partial}{\partial_\tau}\right) \times \left(A(\tau,z)\int_{-\infty}^{\infty} R(\eta)\,|A(z,\tau-\eta)|^2\,d\eta\right), \qquad (1)$$

where A is the field amplitude, $\beta^{(\mathrm{k})} = \partial^{\mathrm{k}}\beta/\partial\omega^{\mathrm{k}}$ are the coefficients in the Taylor-series expansion of the propagation constant β, ω_0 is the carrier frequency, τ is the retarded time, $\gamma = (n_2\omega_0)/(cS_{\mathrm{eff}})$ is the nonlinear coefficient, n_2 is the nonlinear refractive index of the PCF material, $S_{\mathrm{eff}} = [\int_{-\infty}^{\infty}\int_{-\infty}^{\infty}|F(x,y)|^2\mathrm{d}x\mathrm{d}y]^2/\int_{-\infty}^{\infty}\int_{-\infty}^{\infty}|F(x,y)|^4\mathrm{d}x\mathrm{d}y$ is the effective mode area ($F(x,y)$ is the transverse field profile in the PCF mode), and $R(t)$ is the retarded nonlinear response function. For fused silica, we take $n_2 \approx 3.2\cdot10^{-16}$ cm^2/W, and the $R(t)$ function is represented in a standard form [12]:

$$R(t) = (1-f_{\mathrm{R}})\delta(t) + f_{\mathrm{R}}\Theta(t)\frac{\tau_1^2+\tau_2^2}{\tau_1\tau_2^2}\mathrm{e}^{-\frac{t}{\tau_2}}\sin\left(\frac{t}{\tau_1}\right), \qquad (2)$$

where $f_{\mathrm{R}} = 0.18$ is the fractional contribution of the Raman response; $\delta(t)$ and $\Theta(t)$ are the delta and the Heaviside step functions, respectively; $\tau_1 = 12.5$ fs and $\tau_2 = 32$ fs are the characteristic times of the Raman response of fused silica.

To find $\beta^{(\mathrm{k})}$, we numerically solved the Maxwell equations for the transverse components of the electric field in the cross section of a PCF using a modification of the method of polynomial expansion in localized functions, developed by Monro et al. [13]. This generic approach was adapted to

✉ Fax: +7-095-939-3113, E-mail: zheltikov@phys.msu.ru

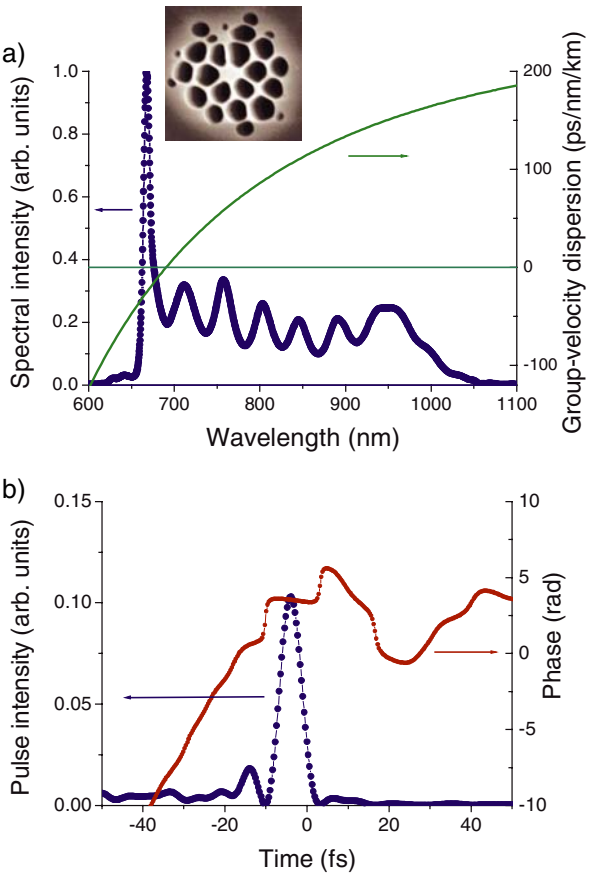

FIGURE 1 **a** Intensity spectrum of the in put laser pulse (Ti:sapphire oscillator output) and group-velocity dispersion of the PCF. The 670-nm peak, dominating the spectrum of the laser pulse, falls within the normal-GVD region of the PCF. The *inset* shows an SEM image of the PCF cross section with a core diameter of 1.6 μm. **b** Temporal envelope and chirp of the Ti:sapphire oscillator output reconstructed from SPIDER data

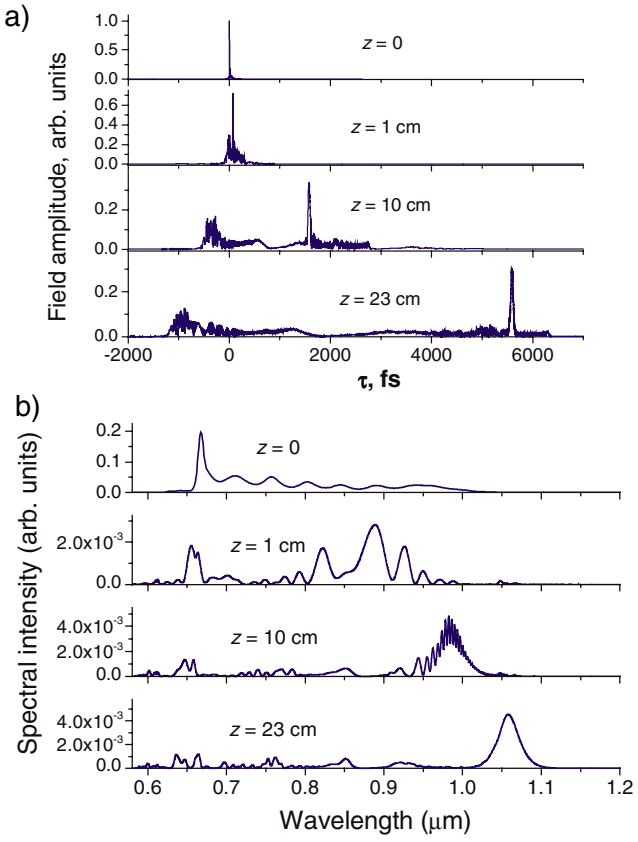

FIGURE 2 Temporal **a** and spectral **b** evolution of a laser pulse with an initial energy of 0.3 nJ and input envelope and chirp shown in Fig. 1a propagating through the PCF

the spatial profile of the refractive index in one of the PCFs employed in our experiments, consisting of a fused silica core with a diameter of 1.6 μm, surrounded with two cycles of air holes (inset in Fig. 1a). Polynomial approximation of the frequency dependence of the propagation constant β for the fundamental mode of the PCF computed with the use of this numerical procedure with an accuracy better than 0.1% within the range of wavelengths from 580 to 1220 nm yields the following $\beta^{(k)}$ coefficients for the central wavelength of 800 nm: $\beta^{(2)} \approx -0.0293\,\mathrm{ps}^2/\mathrm{m}$, $\beta^{(3)} \approx 9.316 \cdot 10^{-5}\,\mathrm{ps}^3/\mathrm{m}$, $\beta^{(4)} \approx -9.666 \cdot 10^{-8}\,\mathrm{ps}^4/\mathrm{m}$, $\beta^{(5)} \approx 1.63 \cdot 10^{-10}\,\mathrm{ps}^5/\mathrm{m}$, $\beta^{(6)} \approx -3.07 \cdot 10^{-13}\,\mathrm{ps}^6/\mathrm{m}$. Figure 1a displays the group-velocity dispersion (GVD) $D = -2\pi c\lambda^{-2}\beta^{(2)}$, where λ is the radiation wavelength, for the fundamental mode of this fibers as functions of the wavelength. The GVD vanishes at $\lambda_z \approx 690$ nm.

Equations (1) and (2) are thus set to compute the evolution of an ultrashort pulse in a PCF. The input temporal envelope and the initial chirp of a laser pulse used as initial conditions in these computations (Fig. 1b) corresponded to the output of the Ti: sapphire laser oscillator employed in experiments presented below in this paper. The input intensity spectrum, shown in Fig. 1a, is dominated by a peak centered at 670 nm. Although this wavelength falls within the normal-GVD range of the PCF (Fig. 1), temporal and spectral evolution of this pulse in the PCF, presented in Fig. 2a and b, respectively, shows that stimulated Raman scattering (SRS) efficiently couples the input energy into a Raman soliton. As can be seen from the frequency-domain dynamics (Fig. 2b), the 670-nm spectral component serves as a pump, efficiently generating a Stokes field through the SRS process. Along with the accompanying spectral broadening effects, SRS nearly totally depletes the most intense part of the input spectrum within a 10-cm section of the PCF.

Because of the anomalous GVD of the PCF, the resulting Raman soliton becomes delayed with respect to the pump pulse (Fig. 2a). As the Raman soliton becomes more and more isolated from the rest of the light field in the time domain, the soliton frequency shift becomes less critically dependent on the fiber length (cf. the results of simulations for $z = 10$ cm and $z = 23$ cm in Fig. 2a and b). Raman solitons isolated in the time domain give rise to well-resolved features in the output spectra, suggesting an attractive strategy for a controlled frequency shifting of extremely short laser pulses to a required spectral range. Figure 2b shows how a sub-6-fs pulse with typical parameters of a Ti: sapphire-oscillator output [14] evolves in a 23-cm piece of PCF to generate a spectrally isolated peak centered around 1064 nm, ideally suited to seed Nd: YAG laser and amplifier components. The increase in the input laser energy gives rise to the formation of multiple Raman solitons and complicates spectral and temporal dynamics of the laser pulse in the PCF. However, with an appropriate choice of the

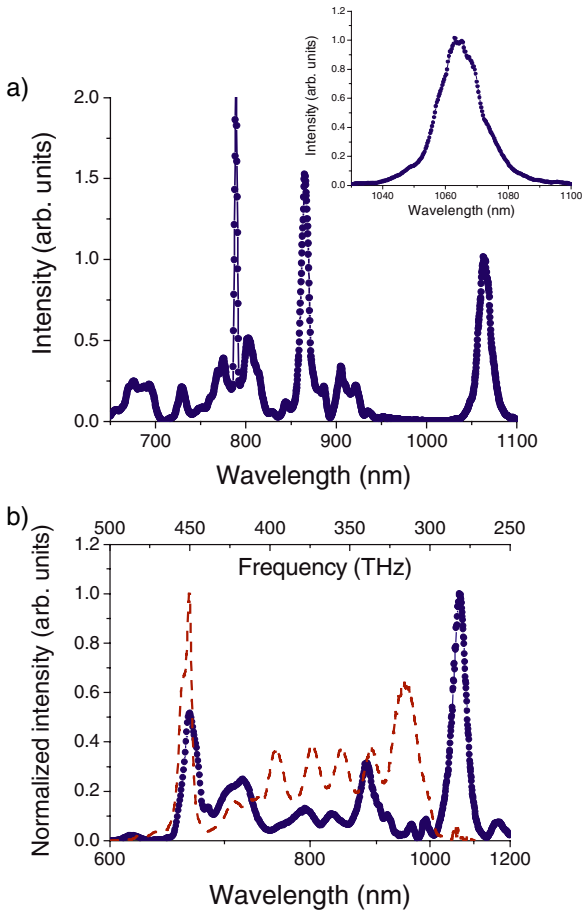

FIGURE 3 Filled circles connected with a *solid line* show experimental spectra measured at the output of **a** a 23-cm PCF with a cross-section structure shown in Fig. 1a and **b** a 20-cm commercial NL-PM-750 fiber. The *dashed line* in Fig. 3b presents the input spectrum, provided by the Ti:sapphire oscillator. The *inset* in Fig. 3a shows the 1064-nm peak in the output of the PCF selected with an interference filter

input energy and the fiber length, intense isolated spectral components at a required wavelength can be produced at the output of the PCF also in this multisoliton regime.

Experiments demonstrating this strategy of ultrashort-pulse frequency shifting in a PCF were performed with a broadband chirped-mirror Ti:sapphire oscillator [14], generating 6-fs pulses with an energy up to 4 nJ at a repetition rate of 70 MHz. The laser output was divided into two channels of roughly equal energies with a beamsplitter. One of the resulting beams was reserved for pumping a Nd:YAG regenerative amplifier [15], while the second beam was sent into the PCF, providing, with allowance for fiber-coupling losses, initial pulse energies in the nano- to subnanojoule range.

The most interesting and practically significant feature of experimental spectra measured at the output of the PCF (Fig. 3a) is the presence of a spectrally isolated peak centered at 1064 nm, as predicted by numerical simulations (cf. Figs. 2b and 3a). This peak is shifted by more than 180 THz with respect to the 670-nm peak, which dominates the input laser-pulse spectrum. An interference filter with a base length of 1.1 μm was used to study this spectral component in greater detail. The result of this investigation is presented in the inset to Fig. 3a. The energy of the 1064-nm output of the PCF selected with the interference filter was about 1 pJ. The contrast of this signal, defined as the ratio of spectral intensities at 1064 nm and 1025 nm exceeded 200. Other peaks observed in the experimental spectrum in Fig. 3a can be attributed to the laser field coupled into higher order guided modes of the PCF. These modes were not included in our model. The spike at 780 nm could originate from cw radiation from the laser oscillator induced by backreflection from the fiber.

To show that the SSFS-based technique of ultrashort-pulse frequency shifting is not specific to a particular PCF design, but is reliably controlled by the dispersion profile, fiber length, and the input energy, we studied the spectral transformation of 6-fs pulses with the above-specified parameters in a commercial NL-PM-750 fiber, manufactured by Crystal Fibre [16]. The core size for this PCF was equal to 1.8 μm, with the first zero-GVD wavelength specified as $\lambda_z = 750$ nm. For this fiber, the main peak in the spectrum of the Ti:sapphire laser output again falls within the range of anomalous dispersion. However, similar to the case of the first PCF, the Ti:sapphire-laser output efficiently couples into the Raman soliton, leading to efficient generation of the spectral component centered at 1064 nm at the output of the fiber. For a 20-cm piece of the NL-PM-750 PCF, the 1064-nm peak was the dominant spectral feature in the PCF output, with its maximum spectral intensity being nearly twice as high as the intensity of the second brightest, 670-nm spectral component.

We have shown in this work that the soliton self-frequency shift in PCFs with a specially designed dispersion profile can provide efficient spectral transformation of few-cycle laser pulses. Experiments presented in this paper demonstrate, in agreement with our numerical simulations, that the spectrum of a 6-fs 2-nJ Ti:sapphire-laser pulse, dominated by a 670-nm peak, is transformed into a spectrum featuring a well-resolved intense spectral component centered at 1064 nm through SSFS in a photonic-crystal fiber with a core diameter less than 2 μm. The signal generated as a result of this spectral transformation is ideally suited as a seed for Nd:YAG- and ytterbium-based laser devices.

ACKNOWLEDGEMENTS We are grateful to K.V. Dukel'skii, A.V. Khokhlov, Yu.N. Kondrat'ev, and V.S. Shevandin for fabricating fiber samples. EES and AMZ acknowledge a partial support of their research by the President of Russian Federation Grant MD-42.2003.02, the Russian Foundation for Basic Research (projects nos. 03-02-16929, 04-02-81036-Bel2004, 04-02-39002-GFEN2004, and 03-02-20002-BNTS-à), INTAS (projects nos. 03-51-5037 and 03-51-5288), and CRDF Award no. RP2-2558.

REFERENCES

1 G.P. Agrawal, *Nonlinear Fiber Optics* (Academic, San Diego, 2001)
2 F.M. Mitschke, L.F. Mollenauer, Opt. Lett. **11**, 659 (1986)
3 E.M. Dianov, A.Ya. Karasik, P.V. Mamyshev, A.M. Prokhorov, V.N. Serkin, M.F. Stel'makh, A.A. Fomichev, JETP Lett. **41**, 294 (1985)
4 P.St.J. Russell, Science **299**, 358 (2003)
5 W.H. Reeves, D.V. Skryabin, F. Biancalana, J.C. Knight, P.St.J. Russell, F.G. Omenetto, A. Efimov, A.J. Taylor, Nature **424**, 511 (2003)
6 X. Liu, C. Xu, W.H. Knox, J.K. Chandalia, B.J. Eggleton, S.G. Kosinski, R.S. Windeler, Opt. Lett. **26**, 358 (2001)
7 I.G. Corrmack, D.T. Reid, W.J. Wadsworth, J.C. Knight, P.St.J. Russell, Electron. Lett. **38**, 167 (2002)
8 D.T. Reid, I.G. Corrmack, W.J. Wadsworth, J.C. Knight, P.St.J. Russell, J. Modern Opt. **49**, 757 (2002)

9 F.G. Omenetto, A.J. Taylor, M.D. Moores, J. Arriaga, J.C. Knight, W.J. Wadsworth, P.St.J. Russell, Opt. Lett. **26**, 1158 (2001)
10 B.R. Washburn, S.E. Ralph, P.A. Lacourt, J.M. Dudley, W.T. Rhodes, R.S. Windeler, S. Coen, Electron. Lett. **37**, 1510 (2001)
11 J.P. Gordon, Opt. Lett. **11**, 662 (1986)
12 K.J. Blow, D. Wood, IEEE J. Quantum Electron. **25**, 2665 (1989)
13 T.M. Monro, D.J. Richardson, N.G.R. Broderick, P.J. Bennet, J. Lightwave Tech. **18**, 50 (2000)
14 T. Fuji, A. Unterhuber, V.S. Yakovlev, G. Tempea, A. Stingl, F. Krausz, W. Drexler, Appl. Phys B. **77**,125 (2003)
15 C.Y. Teisset, N. Ishii, T. Fuji, T. Metzger, S. Köhler, A. Baltuška, F. Krausz, A.M. Zheltikov, *Conference on Lasers and Electro-Optics (CLEO2005)* (Baltimore, ML, 2005), p. 16
16 http://www.crystal-fibre.com/